Available online at www.sciencedirect.com
SCIENCE DIRECT®
Journal of Food Engineering 74 (2006) 431–450
JOURNAL OF FOOD ENGINEERING
www.elsevier.com/locate/jfoodeng

Roller extrusion of biscuit doughs

M.C. Peck [a], S.L. Rough [a], J. Barnes [b], D.I. Wilson [a,*]

[a] Department of Chemical Engineering, University of Cambridge, New Museums Site, Pembroke Street, Cambridge CB2 3RA, UK
[b] United Biscuits Research and Development, Lane End Road, High Wycombe HP12 4JX, UK

Received 21 January 2005; accepted 7 March 2005
Available online 11 May 2005

Abstract

Biscuit doughs are dense solid–liquid pastes which exhibit complex rheological behaviour. The rolling behaviour of sheets of commercial short and hard biscuit doughs was investigated using an instrumented counter-rotating roll mill, which allowed the roll torque, separating force and surface pressure to be monitored. The rheological characteristics of the two doughs were quantified by analysing data from ram extrusion experiments in terms of a quasi-plastic model (following the Benbow–Bridgwater approach) and a power law fluid model. The results indicated that the doughs were not ideally suited to the quasi-plastic analysis. The power law parameters varied noticeably between the doughs but both were strongly shear-thinning (power law shear indices of 0.25 and 0.5), with large extensional viscosities. These rheological model parameters were subsequently used to generate predictions of dough behaviour during rolling. A standard sheet metal plasticity model was modified to include strain rate dependency but neither dough's behaviour could be adequately described by this model. The power law fluid approach based on the lubrication assumption reported by Levine tended to underpredict the work requirement owing to the significant contribution from extensional deformation. Interestingly, the system could be modelled in terms of an apparent power law rheology by fitting data to Levine's model. Better agreement was obtained for some parameters but not consistently so, indicating that the power law approach is not adequate for these soft-solid materials.

Keywords: Dough; Plasticity model; Power law fluid; Rolling

1. Introduction

The sheeting of doughs using roll mills is a prominent operation in the production of both biscuits and bread. In many operations rolling is well understood: the body of literature describing metal sheeting is considerable (e.g. Orowan, 1943); and the rolling of polymer melts, called calendering, has also been studied extensively (e.g. Middleman, 1977). The roller extrusion of food materials such as doughs, however, is a broad area of industrial activity in which current practice still frequently relies on approximations and pilot plant testing. Castell-Perez (1992) and Rao (1992) provide useful introductory accounts of the visco-elastic properties of solid foods, and doughs in particular. They describe the sizeable gap that exists between the material models of practical use in analyses of forming processes, and observations of the complex history dependent response of the materials themselves.

The aim of the current study is to observe and record the behaviour of two contrasting biscuit doughs, i.e. short and hard, in a roll mill. A single pair of smooth rollers of the same size, counter-rotating at the same speed, is thus considered in isolation. As well as qualitative observations, the parameters of interest include the

* Corresponding author. Tel.: +44 1223 334 791; fax: +44 1223 334 796.
E-mail address: diw11@cam.ac.uk (D.I. Wilson).

0260-8774/$ - see front matter © 2005 Elsevier Ltd. All rights reserved.
doi:10.1016/j.jfoodeng.2005.03.033

Nomenclature

a	a power law coefficient [Pa s^b m^{-b}]
b	a power law index [–]
C_f	Levine's roll separating force coefficient [–]
C_{ff}	Levine's finite sheet thickness roll separating force coefficient [–]
C_{fw}	Levine's finite sheet thickness power coefficient [–]
C_w	Levine's power coefficient [–]
D	die land diameter [m]
D_0	extrusion barrel diameter [m]
F	roll separating force [N]
h	vertical roll gap at position x [m]
H	sheet thickness [m]
H_e	exit sheet thickness [m]
H_f	feed sheet thickness [m]
H_0	roll nip dimension [m]
k	shear yield stress [N m^{-2}]
K	power law fluid flow consistency [N m^{-2} s^{λ}]
K_e	power law fluid extensional flow coefficient [N m^{-2} s^{λ}]
L	die land length [m]
L_e	distance between nip and sheet discharge [m]
m	Benbow–Bridgwater die entry velocity index [–]
n	Benbow–Bridgwater die land velocity index [–]
N_{Tr}	Trouton number [–]
p	fluid pressure; roll surface pressure [Pa]
P	total extrusion pressure [Pa]
P_0	pressure drop across die entry region [Pa]
P_s	shear viscosity component of pressure drop [Pa]
P_e	extensional viscosity component of pressure drop [Pa]
Q	volumetric flow rate [m^3 s^{-1}]
q	normal stress within sheet against roller surface [N m^{-2}]
R	roller radius [m]
R^2	Pearson coefficient of correlation [–]
T	roll torque [N m]
u_x	component of fluid velocity in direction of exit sheet [m s^{-1}]
U	roller surface velocity [m s^{-1}]
V	mean extrudate velocity [m s^{-1}]
$\dot{W}$	rate of work input during rolling [N m s^{-1}]
W_0	feed sheet width [m]
x	horizontal coordinate along plane of symmetry from nip [m]
x'	dimensionless x direction = $x/\sqrt{(2RH_0)}$ [–]
y	vertical coordinate perpendicular to roller surface at nip [m]
α	Benbow–Bridgwater yield stress velocity factor [Pa $s^m m^{-m}$]
α'	Benbow–Bridgwater modified yield stress strain rate factor [Pa s^m]
β	Benbow–Bridgwater wall shear stress velocity factor [Pa s^n m^{-n}]
$\dot{\gamma}$	shear strain rate [s^{-1}]
$\dot{\gamma}_{app}$	apparent shear strain rate [s^{-1}]
$\dot{\gamma}_w$	shear strain rate at wall [s^{-1}]
η	apparent shear viscosity [N s m^{-2}]
$\bar{\eta}_e$	average apparent extensional viscosity [N s m^{-2}]
λ	power law fluid flow index [–]
λ'	fluid flow index given by Eq. (6) [–]
Λ	power law fluid extensional flow index [–]
$\dot{\varepsilon}$	extensional strain rate [s^{-1}]
$\bar{\dot{\varepsilon}}$	average or mean extensional strain rate [s^{-1}]
ϕ	angle from nip relative to roll centre [–]
ϕ_e	angular position of exit sheet detachment from roll surface [–]
ϕ_f	angular position of feed sheet contact with roll surface [–]
ϕ_n	angular position of neutral point from nip [–]
Φ	Gibson constant, given by Eq. (9) [–]
μ	viscosity [N s m^{-2}]
θ	die entry angle [–]
σ_0	Benbow–Bridgwater initial die entry yield stress [N m^{-2}]
σ_0'	strain rate adjusted die entry yield stress [N m^{-2}]
σ_y	uniaxial yield stress [N m^{-2}]
τ	shear stress [N m^{-2}]
τ_w	shear stress at wall [N m^{-2}]
τ_0	Benbow–Bridgwater initial paste–die wall shear stress [N m^{-2}]
ω	angular velocity of rollers [s^{-1}]

force exerted by the material tending to push the rollers apart (the roll separating force), the shaft torques required to draw the material into the roll gap, and the profile of the pressure against the roll surface through the roll bite. A particular aim was to establish the extent to which the quantitative characterisation of the dough behaviour, performed here using capillary extrusion, could be applied to modelling the rolling system.

1.1. Characterisation of food doughs

Food doughs are often modelled as power law fluids, representing an approximation to the behaviour of a

wide range of shear-thinning or shear-thickening fluids. Here, the shear stress τ is related to the shear strain rate $\dot{\gamma}$ by the following equation:

$$\tau = K\dot{\gamma}^{\lambda} \tag{1}$$

where K is the consistency of the fluid, and λ is the flow index. Biscuit food doughs are examples of 'soft-solids', namely materials that possess a yield stress but are sufficiently soft to be shaped readily. Soft-solids frequently also exhibit complex flow behaviour, including strain and strain rate dependent responses. Since many soft-solids are multiphase materials, their mechanical behaviour depends on the properties of both the solid and liquid components (Benbow, Lawson, Oxley, & Bridgwater, 1989). Direct prediction of constitutive behaviour is not yet available, and modelling approaches have included the Bingham plastic model (e.g. Ovenston & Benbow, 1967), the power law model, and for materials with a strong strain rate dependency, several workers have used the Herschel–Bulkley model (e.g. Adams, Biswas, Briscoe, & Kamyab, 1991).

In response to the problems encountered when characterising these materials using traditional techniques, Benbow and Bridgwater (1993) developed an approximate method of material characterisation via capillary extrusion. In this approach, the total pressure drop P required to extrude a soft-solid (usually a dense solid–liquid paste) from a circular barrel of diameter D_0 through a concentric circular die of diameter D and length L is given by

$$P = 2(\sigma_0 + \alpha V^m)\ln\left(\frac{D_0}{D}\right) + 4(\tau_0 + \beta V^n)\left(\frac{L}{D}\right) \tag{2}$$

where V is the mean velocity of the material in the die land, i.e. assuming the flow is dominated by wall slip. An average flow rate rather than, for example, an average shear rate, is used because of the dominance of plug flow typical in paste systems. The first term on the right hand side of the equation (termed P_0) represents the work due to the paste undergoing quasi-plastic deformation associated with the contraction; σ_0 is the die entry bulk yield stress of the paste. The second term represents the work due to the shear effects within the die land; τ_0 is the initial paste–die wall shear stress. The parameters α and β, and the indices m and n, are used with V to introduce a strain rate dependence of the yield and shear stresses respectively. Cheyne, Barnes, and Wilson (2005) describe the application of this approach to another example of a food dough, based on potato starch.

The Benbow–Bridgwater approach therefore describes the deformation behaviour of a soft-solid in terms of two distinct properties of the material, viz. the bulk deformational response and the wall slip response. However, if there is no wall slip in the die land, then the Rabinowitsch–Mooney equation for capillary flow of a fluid can be employed to obtain the shear rate at the wall (Steffe, 1992):

$$\dot{\gamma}_w = \frac{3}{4}\dot{\gamma}_{app} + \frac{\tau_w}{4}\frac{d\dot{\gamma}_{app}}{d\tau_w} \tag{3}$$

where $\dot{\gamma}_w$ is the true shear strain rate at the wall, τ_w is the shear stress at the wall, and $\dot{\gamma}_{app}$ is the apparent shear strain rate given in terms of the volumetric flow rate Q and capillary die diameter D by

$$\dot{\gamma}_{app} = \frac{32Q}{\pi D^3} \tag{4}$$

Eq. (3) may be rearranged to yield

$$\dot{\gamma}_w = \dot{\gamma}_{app}\left[\frac{3\lambda' + 1}{4\lambda'}\right] \tag{5}$$

where

$$\lambda' = \frac{d(\ln \tau_w)}{d(\ln \dot{\gamma}_{app})} \tag{6}$$

The parameter λ' may thus be obtained as the gradient of a graph of the logarithm of the wall shear stress plotted against the logarithm of the apparent shear rate. For a power law fluid the plot displays a straight line, and the constant gradient of λ' is equal to the power law flow index λ, as given in Eq. (1).

A promising power law fluid fit in this capillary analysis would suggest that a corresponding calculation for the die entry region during extrusion should also be performed. The key principle behind the analysis is the separating of the die entry pressure drop into two components, the first due to the simple shear viscosity, and the second due to extensional viscosity (Steffe, 1992). The shear viscosity component, P_e, can be calculated using the following expression, the first of the Gibson equations:

$$P_s = \frac{2K(\sin^{3\lambda}\theta)}{3\lambda\theta^{1+3\lambda}}\left(\frac{1+3\lambda}{4\lambda}\right)^{\lambda}\dot{\gamma}_{app}\left(1 - \left(\frac{D}{D_0}\right)^{3\lambda}\right) \tag{7}$$

where θ is the die entry angle. P_s is then subtracted from the total die entry pressure drop, the remainder being the pressure loss due to extensional work. The second Gibson equation estimates this extensional term, P_e, as

$$P_e = (K_e\dot{\gamma}_{app}^{\Lambda}) \times \frac{2}{3\Lambda}\left(\frac{\sin\theta(1+\cos\theta)}{4}\right)^{\Lambda}\left(1 - \left(\frac{D}{D_0}\right)^{3\Lambda} + \frac{\Phi}{4^{\Lambda}}\right) \tag{8}$$

where

$$\Phi = \int_0^{\theta}(\sin^{\Lambda+1}\theta)(1+\cos\theta)^{\Lambda-1}\,d\theta \tag{9}$$

and where K_e is the power law extensional flow coefficient and Λ is the power law extensional flow

index. The average extensional strain rate for flow into the die land is given by

$$\bar{\dot{\varepsilon}} = \frac{\dot{\gamma}_{app} \sin\theta(1+\cos\theta)}{4} \tag{10}$$

and the average apparent extensional viscosity is given by

$$\bar{\eta}_e = K_e \bar{\dot{\varepsilon}}^{A-1} \tag{11}$$

The Trouton number, N_{Tr}, is often quoted as a measure of the ratio between (the apparent) extensional viscosity and (the apparent) shear viscosity η, and is thus a function of strain rate. For uniaxial flow it is conventional to evaluate the apparent shear viscosity at a strain rate of $\sqrt{3}$ times the extensional strain rate, as follows:

$$N_{Tr} = \frac{\bar{\eta}_e(\bar{\dot{\varepsilon}})}{\eta(\sqrt{3}\bar{\dot{\varepsilon}})} \tag{12}$$

Thus high values of N_{Tr} indicate that extensional terms are likely to dominate in any deformation comprising both shear and extensional strain components.

1.2. Modelling of rolling

Calendering of polymers has been studied extensively and this process is depicted schematically in Fig. 1(a). A basic analysis is presented by Middleman (1977), in which the polymer is treated as a Newtonian liquid. The flow is assumed to be perfectly two-dimensional and inertial terms are neglected. Furthermore, the process is assumed to be dominated by conditions at the nip region, where the curvature of the rollers is insignificant. The flow in this region will thus be nearly parallel, and hence the problem may be reduced to that of Reynolds lubrication. This enables the horizontal fluid velocity, u_x, to be found in terms of the vertical coordinate y and the pressure gradient dp/dx. Applying non-slip boundary conditions at the roller surface and symmetry across the centre plane yields

$$u_x = U + \frac{y^2 - h^2(x)}{2\mu}\frac{dp}{dx} \tag{13}$$

where U is the roller surface velocity, μ is the fluid viscosity, and $h(x)$ represents the shape of the roller surface. Middleman approximated the roller surface in the region of interest (i.e. the roll nip) as a parabola. The analysis proceeds by manipulating Eq. (13) to obtain an expression for dp/dx in terms of the volumetric flow rate, which is then integrated to obtain p. The boundary conditions used by Middleman were that both $dp/dx = 0$ and $p = 0$ as the sheet leaves the rollers (implying that the flow is perfectly parallel and uniform at that point), and that $p = 0$ far upstream in the polymer melt. This has the interesting effect of predicting a swell of the sheet beyond the roll nip before it detaches from the rollers, shown schematically in Fig. 1(a). The problem is thus essentially solved, producing algebraic expressions for p, u_x and important process parameters such as the roll torques and separating forces.

Numerous modifications have since been added to this analysis. For example, in 1978 Kiparissides and Vlachopoulos reported the development of the temperature profile for a power law fluid using an early finite element method. By 1983, Chung included the effect of compressible melts, and in 1985 Mitsoulis, Vlachopoulos and Mirza published a complete two-dimensional finite element solution. The calendering analysis has also been extended to the rolling of dough sheets (e.g. Levine, 1983, 1985, 1996). Few foodstuffs behave as Newtonian liquids, so a more sophisticated rheological model was required, and Levine and Drew (1990) present a complete summary of the rolling of dough sheets modelled as power law fluids. The theoretical construction is identical to that of the basic calendering analysis, except for adjustments to pressure boundary conditions (zero at the feed sheet roll contact rather than far upstream) and the underlying constitutive equation. A circular roll surface profile is used rather than the parabola approximation. Large parts of the calculation involve numerical integration, but they parameterise the solutions and provide graphical charts so their

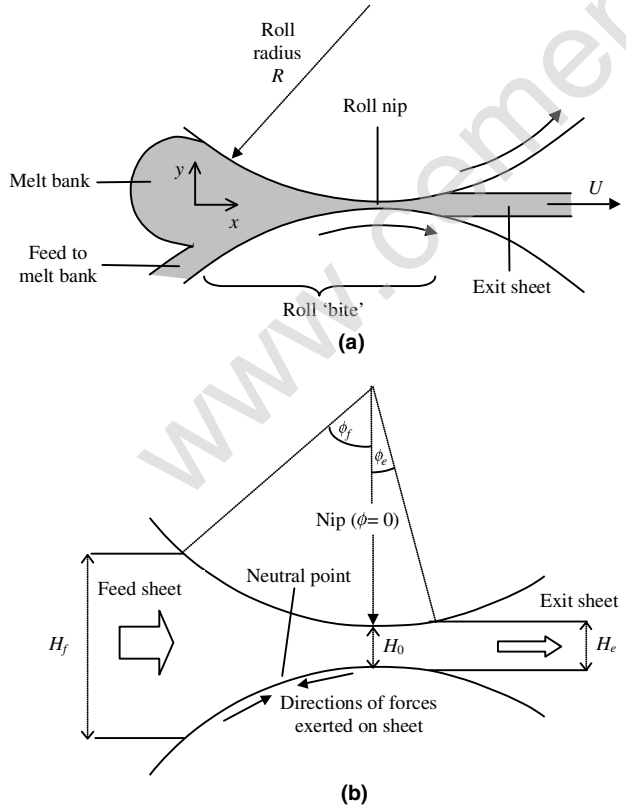

Fig. 1. Cross-section of the (a) polymer calendering process and (b) hot metal rolling process, with descriptive terms used.

solutions may be readily applied to fluids with a range of values for K and λ in Eq. (1). The subsequent equations for work input rate $\dot{W}$ (which may be used to calculate roll torque), roll separating force F, and roll surface pressure p, are as follows:

$$\dot{W} = W_0 U^2 K \left(\frac{U}{H_0}\right)^{\lambda-1} \sqrt{\frac{R}{H_0}} C_w(\lambda) C_{fw}(\lambda, H_f/H_0) \tag{14}$$

$$F = W_0 K \left(\frac{U}{H_0}\right)^{\lambda} R C_f(\lambda) C_{ff}(\lambda, H_f/H_0) \tag{15}$$

$$p = K\left(\frac{U}{H_0}\right)^{\lambda}\left(\frac{2\lambda+1}{\lambda}\right)^{\lambda} \times \sqrt{\frac{2R}{H_0}}\left[\int_{x'}^{L_e} \frac{(L_e^2 - x'^2)^{\lambda}}{(1+x'^2)^{1+2\lambda}}\,dx'\right] \tag{16}$$

where W_0 is the feed sheet width, H_0 is the roll nip dimension, R is the roller radius, H_f is the feed sheet thickness, L_e is the distance between the nip and the sheet discharge, and x' is the dimensionless distance $x/\sqrt{(2RH_0)}$. Levine and Drew's graphs provide values for the coefficients C_w, C_{fw}, C_f and C_{ff} for flow indices λ of between 0.1 and 1, and for reductions of up to 90%. It is noteworthy that the coefficients which account for the finite sheet thickness (those with double subscripts) are highly significant. For values of λ of around 0.25, for example, multiplication by the coefficient C_{fw} reduces estimates for the power consumed by a factor of 10 or more. The roll separating force is not affected quite so markedly, with the finite thickness prediction being at most half that predicted by the calendering model. Levine (1996) thus characterises dough sheets by finding values for K and λ which give a reasonable fit to his equations.

Different modelling approaches are required for plastic materials, dominated by deformation and yield stress behaviour. In a previous study (Peck, Rough, & Wilson, in press), the plasticity-based hot metal rolling analysis of Orowan (1943) was used to describe the rolling behaviour of a stiff ceramic paste with moderate success. In hot rolling, the bulk yield stress is sufficiently low that the sheet and rollers tend to be in sticking contact. It is appropriate to treat the sheet as leaving the rollers at the nip ($\phi = 0$) and unlike the calendering of polymers, the sheet does not expand significantly beyond it (Fig. 1(b)). In the present experiments, the measured exit sheet thickness was slightly larger than the estimated nip separation (e.g. by up to 6%), which could be the result of elastic effects. However, such elastic effects are not considered in the modelling here. The analysis considers the stress distribution within an arc of material running from the roller to the centre line of the sheet, by assuming that the entire arc is at the yield point. The position of the neutral point, where the tangential forces at the roller surface are equal and opposite (at $\phi = \phi_n$), determines the roll torque T:

$$T = W_0 k R^2 (\phi_f - 2\phi_n) \tag{17}$$

where k is the shear yield stress of the material, and ϕ_f represents the point of first contact of the sheet with the rollers. The roll separating force is given by

$$F = W_0 R \int_0^{\phi_f} q\cos\phi\,d\phi + W_0 R k\left(\int_{\phi_n}^{\phi_f} \sin\phi\,d\phi - \int_0^{\phi_n} \sin\phi\,d\phi\right) \tag{18}$$

where q is the normal stress against the surface of the roller.

2. Experimental methods

2.1. Dough preparation

The materials studied were two contrasting food doughs provided by United Biscuits (High Wycombe, UK). The main ingredients of both doughs are wheat flour, fat and sugar. The first material is a type of 'short dough', so named because of its relatively high percentage of fat (25–30 wt.% of the flour, or more), which acts to tenderise or 'shorten' the dough (Bennion, 1980). Short doughs are relatively crumbly materials, and are poorly cohesive and fairly inelastic (Podmore, 1994). The second material is more elastic and glutinous, and represents an example of a 'hard dough'. Hard doughs contain less fat and are mixed more aggressively to develop the three-dimensional gluten network of the dough.

An important constituent of these doughs is fat, featuring a range of melting points which bracket the ambient temperatures at which the experiments in this study were performed (Gisslen, 2001). The physical characteristics of the doughs were thus temperature dependent, and some results of tests investigating the extent of this are presented in Section 2.2.1. The 'ageing' of doughs is commonly observed (Gisslen, 2001), and was found to be significant over the time scale of experimental work performed in this study.

2.1.1. Short dough

Batches of 1 kg of dough were prepared in a domestic Kenwood 'Chef' planetary mixer according to supplied instructions. This involved 'creaming' together the butter, sugar and water components before adding the flour and mixing at a slower speed in a multi-stage mixing process. Great care was taken to follow the same procedure for all batches of material. Mixing time is widely regarded as having a pronounced effect on the rheological characteristics of doughs (e.g. Manohar & Rao,

1997), and particular attention was paid to this parameter. The dough was subsequently required to stand for 30 min. The low speed mixing did not produce significant quantities of heat, and the prepared dough remained at room temperature. Despite being stored in an airtight plastic bag, the material behaviour was found to alter with time, even within the time scale of experimental work. All rolling experiments were therefore completed as soon as possible after the specified standing period.

2.1.2. Hard dough

Batches of 1.4 kg of dough were prepared in a Morton Z-blade mixer according to supplied instructions. The mixing process was longer and more aggressive than that of the short dough, and the product obtained was somewhat warmer than ambient. The required standing time was 5 min and the subsequent rapid change of dough characteristics with time demanded that experiments be conducted as soon as possible after mixing was complete, with the recommended maximum age being 30 min.

2.2. Dough characterisation

The doughs were characterised primarily with the Benbow–Bridgwater method, and the procedure adopted was similar for both materials. A circular steel barrel of 25 mm internal diameter was loaded with dough. The material was then ram extruded through concentric square entry circular dies of diameter 3 mm and lengths 6, 12, 24, 36 and 48 mm. In each test with a given die, the piston was stepped through eight different speeds using a Dartec SA100 strain frame. Assuming the doughs to be incompressible, the ram speeds of between 0.016 and 0.833 mm s^{-1} produced mean extrudate velocities V of between 1.1 and 57.8 mm s^{-1}, and apparent die land shear strain rates $\dot{\gamma}_{app}$ of between 3 and 154 s^{-1} (as given by Eq. (4)). Prior to extrusion, the short dough samples were compacted to an average normal stress of 2 kPa to remove air voids; concern over the time sensitivity of the hard dough demanded that this step be omitted for this material.

2.2.1. Short dough

The die entry pressure P_0 for short dough, obtained via extrapolating extrusion data to zero die length L, is depicted in Fig. 2(a). Plotting the values on logarithmic axes indicated that the data could be well represented by a relation of the form $P_0 = aV^b$. Comparison with Eq. (2) indicates that this corresponds to the Benbow–Bridgwater model in which the yield stress term σ_0 is zero. However a zero yield stress is not consistent with observations, in that the dough is found to have strength sufficient to maintain its shape for a number of hours when formed into a block. However, if the range and associated error bars are considered, then the spectrum of lines satisfactorily fitting the data could correspond to a range of plausible values for σ_0. Sets of parameters were calculated by assuming fixed values for σ_0 and finding optimum values for α and m (Table 1). It was found that values of σ_0 in the range of 0 to about 0.1 MPa fitted the data well.

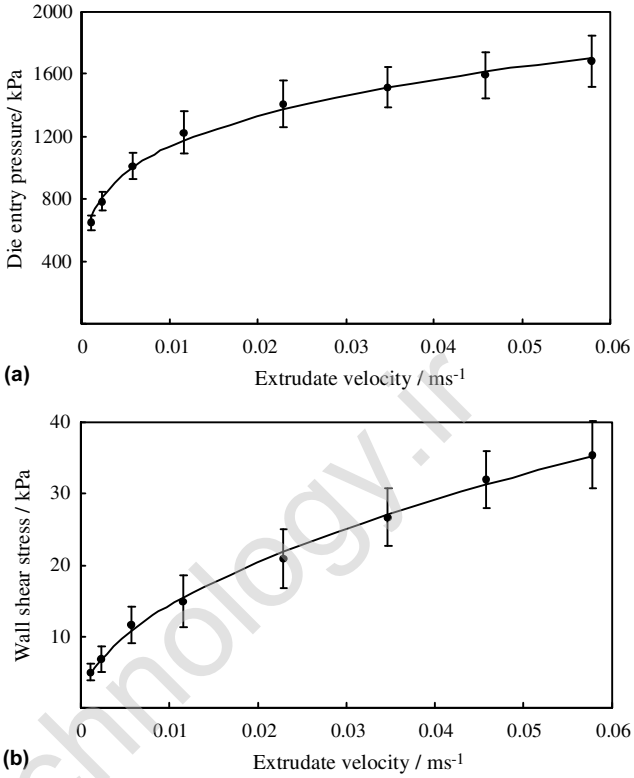

Fig. 2. (a) Die entry pressure and (b) die land wall shear stress for ram extrusion of short dough. Solid lines represent fits given by characterisation parameters listed in Tables 1 ($\sigma_0 = 0$) and 2.

The die wall shear stress term $(\tau_0 + \beta V^n)$ for short dough, obtained via the Benbow–Bridgwater characterisation process, is shown in Fig. 2(b). The figure also shows the three-parameter expression obtained by regression; the parameters are listed in Table 2. The Benbow–Bridgwater analysis assumes that shearing of the dough occurs only at the die wall. However, internal shearing may be expected as the wall yield stress approaches the shear yield stress of the dough. Horrobin (1999) provided a relation for the uniaxial yield stress for this system, $\sigma_y \approx 0.82\sigma_0$ (assuming in this case that the extrusion pressure does not depend upon the extrudate velocity). Applying a von Mises yield criterion, the plug flow assumption would therefore be valid if

$$\frac{0.82}{\sqrt{3}}\sigma_0 > (\tau_0 + \beta V^n) \tag{19}$$

Employing a value of $\sigma_0 = 0.1$ MPa, then internal shearing is unlikely, even at the highest extrudate velocity. The wall yield stress term rises to about 80% of the bulk

Table 1
Benbow–Bridgwater characterisation parameters for the die entry region of short and hard doughs, with $\sigma_0 = 0$, 0.04, 0.08, 0.16 and 0.24 MPa

	σ_0/MPa				
	0	0.04	0.08	0.16	0.24
Short					
α/MPa (m s^{-1})$^{-m}$	0.78 ± 0.17	0.79 ± 0.19	0.82 ± 0.23	1.13 ± 0.41	–
m	0.23 ± 0.04	0.27 ± 0.04	0.33 ± 0.06	0.53 ± 0.07	–
R^2	0.9937	0.9905	0.9848	0.954	–
Hard					
α/MPa (m s^{-1})$^{-m}$	1.56 ± 0.28	1.58 ± 0.30	1.62 ± 0.33	1.78 ± 0.38	2.18 ± 0.60
m	0.26 ± 0.03	0.28 ± 0.04	0.31 ± 0.04	0.38 ± 0.05	0.50 ± 0.06
R^2	0.9868	0.9866	0.9859	0.9824	0.9725

Table 2
Benbow–Bridgwater characterisation parameters for the die land behaviour of short and hard doughs

	Short	Hard
τ_0/MPa	0.002	0.008
β/MPa (m s^{-1})$^{-n}$	0.18 ± 0.004	0.090 ± 0.008
n	0.58 ± 0.01	0.58 ± 0.33
R^2	0.9979	0.8597

Table 3
Power law parameters, obtained using the Rabinowitsch–Mooney analysis, for the shear response of short and hard doughs

	Short	Hard
K/kPa s$^{\lambda}$	2.55 ± 0.70	6.3 ± 2.5
λ	0.5 ± 0.1	0.25 ± 0.12
R^2	0.9975	0.9240

shear yield stress. However, given the level of uncertainty in σ_0, one may conclude that internal shearing could be having an influence, and so an alternative characterisation approach, such as that of capillary analysis, must be considered.

The Rabinowitsch–Mooney plot of the logarithm of the wall shear stress against the logarithm of the apparent shear rate for short dough is shown in Fig. 3. If there is indeed no wall slip, then the short dough does appear to be flowing as a shear-thinning power law fluid with a value of λ, given by the gradient of the best fit line, of 0.5 ± 0.1. Inserting this value into Eq. (3) via Eqs. (5) and (6), since $\lambda = \lambda'$ for a power law fluid, yields the shear rate at the wall. Since the shear stress at the wall is also known, the power law constant K can be calculated for the dough in simple shear (Table 3).

One problem with the Gibson analysis outlined in Section 1.1 is the uncertainty of the die entry angle θ,

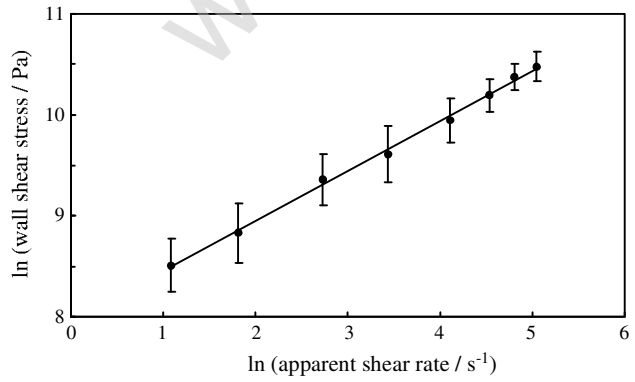

Fig. 3. Rabinowitsch–Mooney plot for short dough. Solid line represents best fit power law trendline.

since static zones form in the corners of square entry dies during extrusion. Die entry angles of 45° and 60° were used as examples in the analysis here. Values for Λ and K_e were obtained by plotting $\ln(P_e)$ against $\ln(\dot{\gamma}_{app})$. By Eq. (8), Λ is obtained from the gradient while K_e is obtained from the intercept, and these parameters are listed in Table 4. The fit is not quite as good as in the capillary analysis, as reflected by the lower R^2 value of 0.9934. The variation of K_e and Λ with die entry angle is shown in Fig. 4. Λ is found to be relatively insensitive to die entry angle, whereas K_e is rather more dependent, varying by 50% over the most likely range of interest, 45–90°.

From Eq. (10), the average extensional strain rate for flow into the die land varies between 36 and 0.7 s^{-1}, and the average apparent extensional viscosity, given by Eq. (11), thus varies between 20,000 and 400,000. Hence Eq. (12) gives the Trouton number, the values of which are given in Table 4, and the high values indicate that extensional terms are likely to dominate any deformation comprising both shear and extensional components over this range.

The reproducible extrusion results permitted an investigation of the effects of dough temperature and age using the ram extruder. For the effect of dough temperature, tests were run with a very short die ($L/D = 2$) so that die land temperature dependence would not obscure the response of the extensional deformation of the die entry region. As the temperature was increased from 17 to 25 °C, the pressure necessary to extrude the dough at a velocity of 0.058 m s^{-1} decreased in a linear manner from 2.2 to 1.3 MPa. No further decrease in pressure was observed between 25 and 27 °C. This significant

Table 4
Power law parameters, obtained using the Gibson equations, for the extensional response of short and hard doughs

	Short		Hard	
	60°	45°	60°	45°
K_e/kPa s^{Λ}	240 ± 15	271 ± 15	440 ± 18	492 ± 18
Λ	0.24 ± 0.04	0.24	0.26 ± 0.03	0.26 ± 0.03
N_{Tr}	45–124	51–141	89–108	100–133
R^2	0.9934	0.9934	0.9912	0.9910

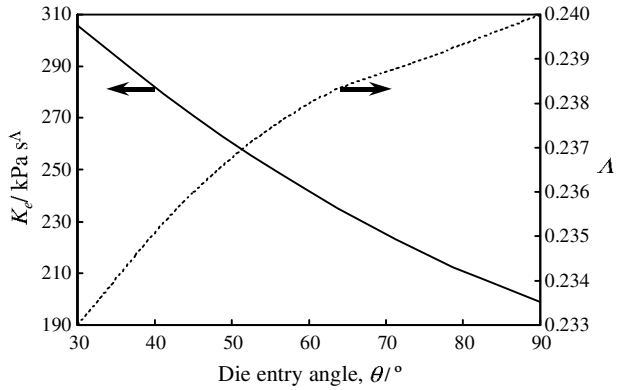

Fig. 4. Influence of die entry angle θ on power law extensional flow coefficient K_e (solid line) and power law extensional flow index Λ (dotted line) in Gibson analysis.

change of mechanical properties prompted a calorimetric study of the dough. The cooling profile from a Differential Scanning Calorimeter (PerkinElmer Pyris1) displayed a small peak corresponding to a phase change between approximately 23 and 18 °C. The heating curve showed a peak in this temperature range but it was less distinct. These effects are related to the fat components in the dough, which exhibit a distribution of melting points in this temperature range (the hard dough also showed a similar response).

The dependence of extrusion pressure on short dough age is shown in Fig. 5. The results confirmed that dough ageing has a significant influence on its physical properties, displaying an apparently linear increase with dough age.

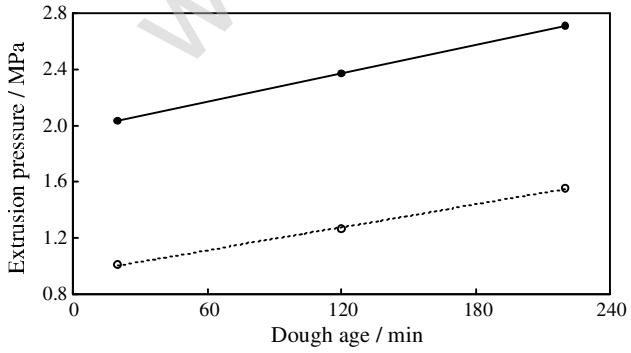

Fig. 5. Dough age dependence of extrusion pressure for short dough through two die lengths: L = 3 mm (open symbols) and L = 24 mm (closed symbols); die diameter = 3 m, extrudate velocity = 0.058 m s^{-1}.

2.2.2. Hard dough

Extrusion of the hard dough was found to be much more erratic than that of the short dough. Most notably, there was a significant increase in extrusion pressure for a given piston speed over the course of an experiment, which is consistent with extrusions in which the liquid phase has migrated (Rough, Bridgwater, & Wilson, 2000). There was some evidence of this in the high levels of a greasy discharge observed around the compact of dough remaining in the barrel at the end of each test. The unusual response of the material may also be due to its greater elasticity and compressibility. Despite this inconsistency, an attempt was made to characterise the dough.

The die entry pressure drop over the range of extrudate velocities is shown in Fig. 6(a). This is qualitatively similar to that for short dough (Fig. 2(a)) in being non-linear and quantifiable by a range of parameters as shown in Table 1. Values for m lie over a similar range to those obtained for the short dough, whilst those for α are roughly double the corresponding values for short dough.

The wall shear stress dependence on extrudate velocity for hard dough shown in Fig. 6(b) is unusual, although the scatter in the experimental data causes large uncertainties in the values. It appears to exhibit a two-part response, rising sharply at low velocities and then crossing a transition to a slower increase at an extrudate velocity of about 6 mm s^{-1}. A particularly broad range of parameters fits this data, albeit not very well. Table 2 shows an example of such a fit.

As with the short dough, it is unclear whether the dough will be exhibiting plug flow in the die land or internally shearing. The slightly stiffer nature of the hard dough increases the likelihood of plug flow but the spread of the findings makes it impossible to draw any firm conclusions. Therefore the results of a capillary analysis are still presented, and used to estimate the extensional viscosity as in Section 2.2.1. A reasonable straight line fit was obtained for the Rabinowitsch–Mooney plot, although the errors bars permitted a wide range of possible power law constants, the average of which are listed in Table 3. A plot of ln(P_e) against

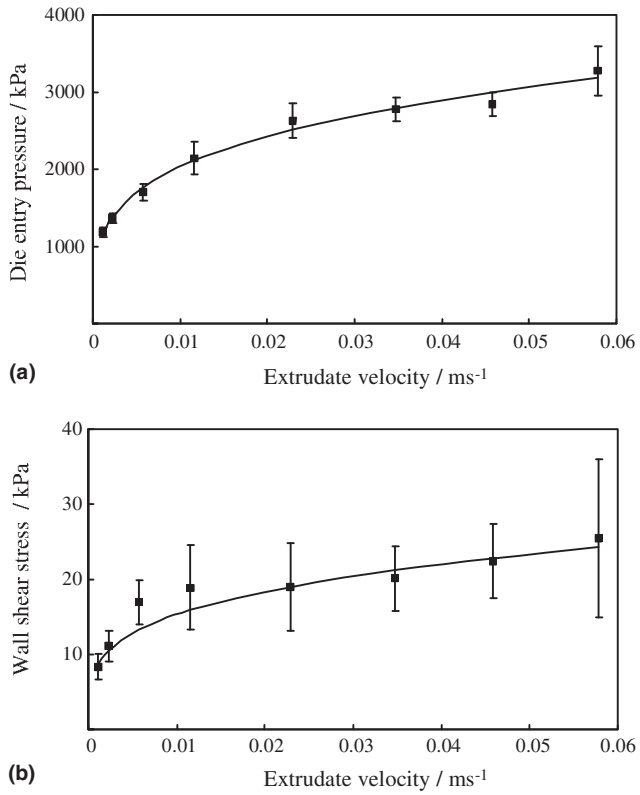

Fig. 6. (a) Die entry pressure and (b) die land wall shear stress for ram extrusion of hard dough. Solid lines represent fits given by characterisation parameters listed in Tables 1 ($\sigma_0 = 0$) and 2.

$\ln(\dot{\gamma}_{app})$ yielded values for Λ and K_e as listed in Table 4. Varying the die entry angle from 30° to 90° had no significant effect on Λ, while K_e was found to vary correspondingly between 0.56 and 0.36 MPa $s^{-\Lambda}$.

2.3. Dough feed sheet preparation

A number of rectangular dough feed sheets of uniform thickness were prepared by hand-rolling appropriate quantities of dough between brass strips of a known height (2.34–9.60 mm). Details of the procedure are given by Peck et al. (in press). The feed sheets were trimmed with a scalpel to a width of 100 mm, which was the maximum practical width given the length of the motor-driven rollers. In general, experiments were designed so that the output sheets were 80–100 mm in length, which allowed for a steady state to be reached during rolling. No feed sheet was used more than once.

2.4. Rolling apparatus and experiments

A schematic plan of the rolling apparatus is shown in Fig. 7. Full details of its components are described elsewhere (Peck, 2002). The apparatus comprises an electric motor driving two counter-rotating shafts connected by directly intermeshing cog-wheels. Each shaft is fitted with a brass roller of diameter 100 mm and length 110 mm. The distance between the rollers can be altered up to a maximum of 40 mm (±0.1 mm). Each drive shaft is fitted with a 20 N m torque transducer. Roller 1 is mounted on moveable framework, and Roller 2 is mounted on framework held in place with a 5 kN load cell. An optical sensor is located at the end of Roller 1 which allows for precise calculation of the orientation of the rollers (±0.004 rad) relative to the roll nip. A 100 kPa piezoelectric pressure sensor is embedded within the surface of Roller 2. The experimental uncertainty of the roll torque measurements was estimated as ±0.2 N m, and that of the roll separating force as ±5 N.

In each experiment the gap between the rollers was adjusted and the rollers started and set to the desired speed. The feed sheet was held just above the roll nip and then released, passing between the rollers under its own weight. For the short dough experiments, reproducibility required completely clean roller surfaces for each test. The elastic and cohesive nature of the hard dough left the rollers relatively clean after each test, with only a light greasy residue remaining; the roller surface cleanliness was found to have no clear effect on roll torques or separating forces.

Experiments were conducted with a range of feed sheet sizes as described in Section 2.3, which were reduced in thickness by 3–78%, at three rotation speeds of 1.5, 6 and 20 rpm (±2%). Further experiments were conducted in which only the roller speed was varied, by increments between 1.5 and 30 rpm, and experiments were also performed to test explicitly the effect of dough age. Sheet width was measured with a ruler to the nearest millimetre. Average feed sheet thickness (±5%) and output sheet thickness (±0.2 mm) were measured using callipers. Experiments in which lateral spread, determined by measurement of the width of the feed and exit sheets, was greater than 10% were abandoned.

3. Experimental results

3.1. General observations

About 90 rolling experiments were completed for each dough. The short dough sheets tended to crumble or disintegrate during rolling. Because of the handling problems associated with these relatively weak sheets, very few experiments were completed with the thinnest sheet size (nominally 2.3 mm). In at least 15% of the short dough tests the product sheet disintegrated or fractured. In the two most severe cases, surface friction was too low to roll the sheet. Instead, small fragments about 1 cm square were continually broken off and rolled separately whilst the feed sheet oscillated from side to side at the entry to the roll bite. In other cases the sheet disintegrated in the gap between the rolls. Light surface

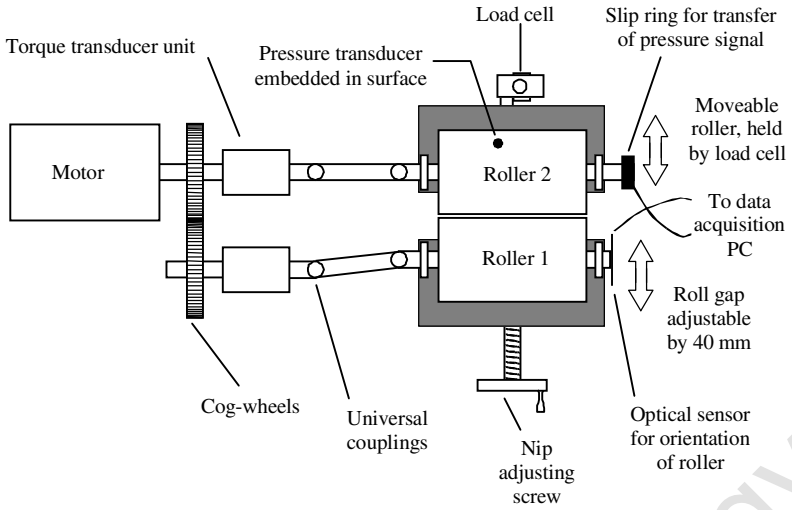

Fig. 7. Schematic plan view of roller extrusion apparatus.

fracturing of the product sheet tended to occur for reductions of between 15% and 30%, whilst the more severe disintegration tended to occur when reductions greater than 65% were attempted.

At the roll exit, the short dough sheets adhered to one or both roller surfaces for reductions greater than 13%. However, this adhesion did not have a significant influence on the average roll torque or roll separating force. The hard dough sheets did not crumble or disintegrate during rolling; the well-developed gluten network caused the sheet to remain intact. The sheets adhered lightly to one roller in nearly all of the experiments, and were easily peeled away. Once again, this adhesion did not have a significant effect on the average roll torque or roll separating force.

3.2. Roll torque and separating force

Sample traces of the average roll torque (i.e. the average of the sum of the torques monitored by Roller 1 and Roller 2) and roll separating force for short dough are shown in Fig. 8. The average fluctuation in these values about a mean was found to be 17% and 10% respectively. The average difference between the two roller torques was about 65% of the average overall torque. For hard dough, the average fluctuation in the roll torque and separating force was found to be 10% and 15% respectively. In general the traces were less noisy than those of the short dough, as might be expected from a dough with a smoother texture. The maximum difference between the two roller torques was 63% of the average, i.e. similar to that for short dough.

The steady state values of the average roll torques and roll separating forces at a nominal roller speed of 6 rpm are shown in Fig. 9 as functions of exit sheet thickness (H_e) for short dough. In general the trends in the rolling parameters are linear (also seen for hard

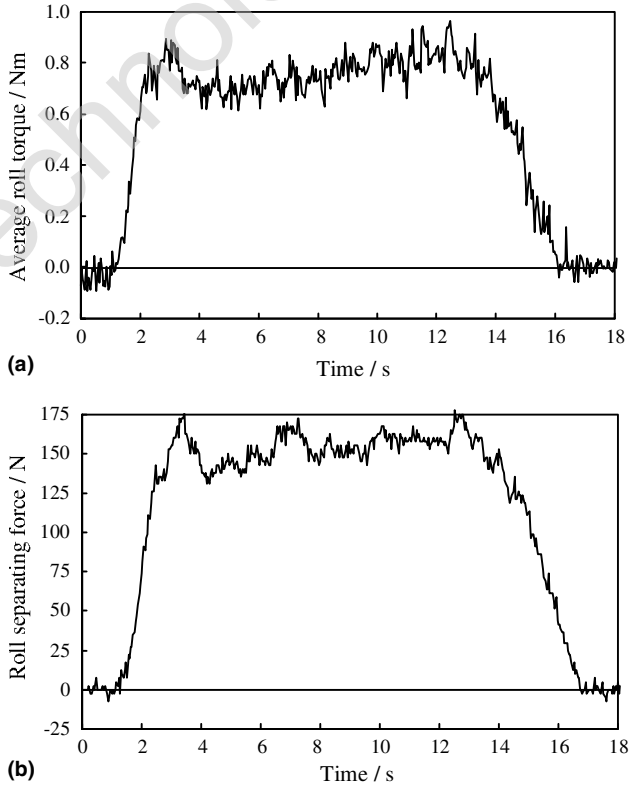

Fig. 8. (a) Average roll torque and (b) roll separating force as a function of time for the rolling of short dough at 1.5 rpm. Feed sheet thickness = 2.8 mm, exit sheet thickness = 0.8 mm.

dough), and similar trends were obtained at speeds of 1.5 and 20 rpm (data not reported here). Plots of the average roll torque and roll separating force at 6 rpm against the reduction ratio (defined as the ratio of exit to feed sheet thickness, H_e/H_f) are shown in Figs. 10 and 11 for both doughs. For the short dough, the roll separating force exhibits a linear relationship for most of the values, whereas the average roll torque data show

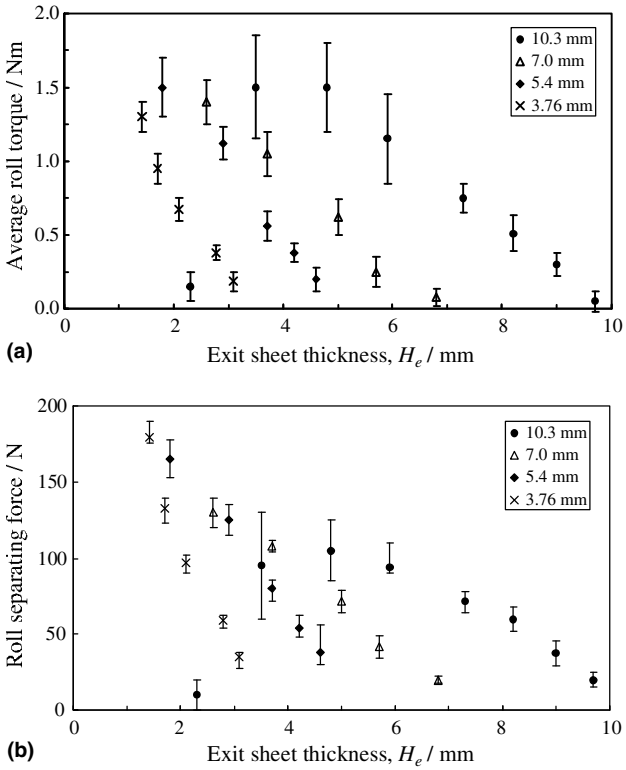

Fig. 9. Steady state values of (a) average roll torque and (b) roll separating force as a function of exit sheet thickness for the rolling of short dough at 6 rpm, for feed sheet thickness ranging from 10.3 to 4.0 mm as indicated in the legends. Error bars represent fluctuation in parameter about steady state mean value.

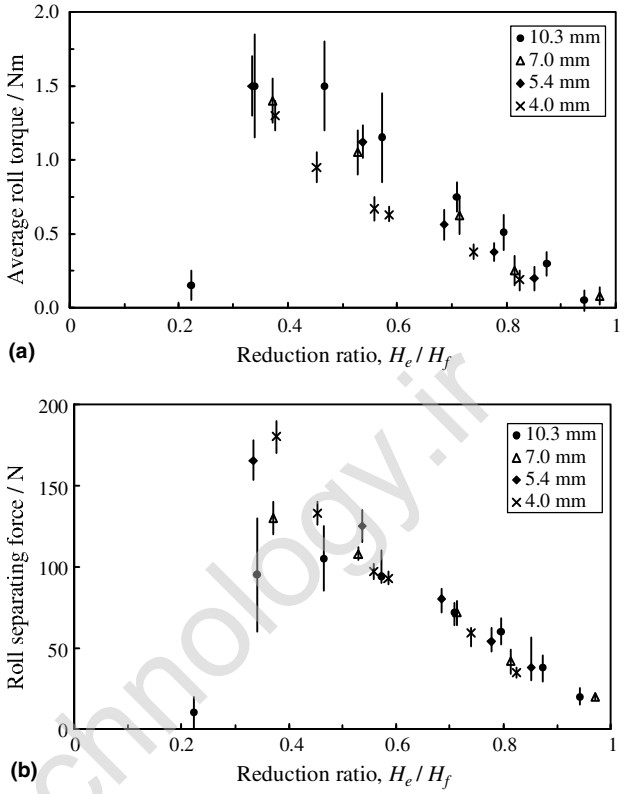

Fig. 10. Steady state values of (a) average roll torque and (b) roll separating force as a function of sheet reduction ratio (H_e/H_f) for the rolling of short dough at 6 rpm, for feed sheet thickness ranging from 10.3 to 4.0 mm as indicated in the legends.

a slight spread. Only the very largest reduction in thickness failed to produce a coherent sheet, and the average roll torque and separating force values are correspondingly low. The trends in the data for the hard dough display an opposite effect, i.e. the average roll torque data follow a linear trend, whereas the roll separating force data show some scatter.

3.3. Pressure profiles

Some typical pressure profiles obtained during the rolling of short and hard doughs are shown in Fig. 12. The profiles featured for the short dough did not exhibit significant levels of sheet breakage or fracture, and yet two pressure peaks develop as the roll separation decreases. One possible cause of this may be a recirculating flow pattern at the bite entry. In the calendering of polymers, zones of recirculation are identified in the melt bank (e.g. Mitsoulis, Vlachopoulos, & Mirza, 1985). To the nip side of the recirculation pattern the material is predicted to be flowing away from the roller surface, and to the entry side it is flowing towards the roller. As the sheet reduction increased, material started accumulating at the roll gap entry, adding further evidence in support of this proposition. Some pressure profiles showed a small step (between 20 and 40 kPa) at the initial contact between sheet and roller, and also exhibit negative roll surface pressures at the sheet exit (mostly between −10 and −15 kPa).

For the hard dough experiments, small humps are evident near the entry region in two of the pressure traces, but in general such features were not as prominent as in the short dough experiments; in the cases where they were observed they occurred at a wide variety of pressures, ranging between 20 and 100 kPa. Whilst the short dough exhibited negative pressures at the exit region in some experiments, the hard dough did not feature this phenomenon. This is thought to be due to the more elastic, compressible nature of the material. Fig. 12(b) includes traces from experiments in which the product sheet adhered to the roller with the pressure transducer; in these tests the transducer records a positive (compressive) force after rolling has finished.

3.4. Age, speed and temperature dependence

Experiments were performed using short and hard doughs to establish the extent to which the average roll torque and roll separating force were affected by dough age, and the results are shown in Fig. 13. For the short

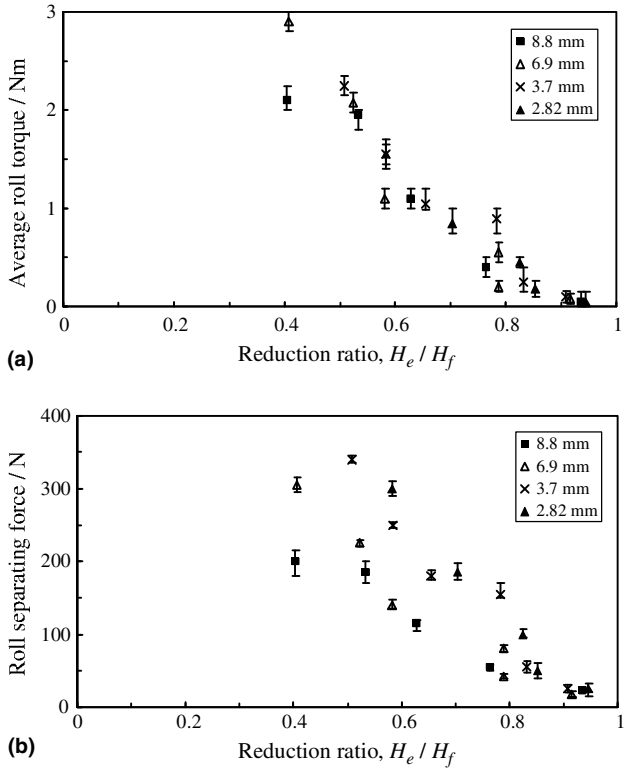

Fig. 11. Steady state values of (a) average roll torque and (b) roll separating force as a function of sheet reduction ratio (H_e/H_f) for the rolling of hard dough at 6 rpm, for feed sheet thickness ranging from 8.8 to 2.8 mm as indicated in the legends.

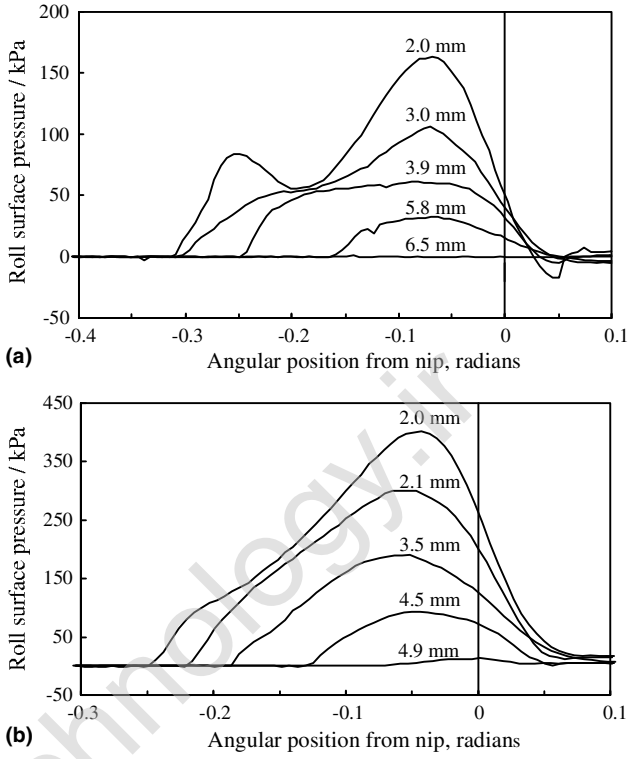

Fig. 12. Roll surface pressure profiles as a function of angular position from nip (positive towards roll exit) at 20 rpm: (a) short dough, feed thickness = 7.2 mm, exit thickness ranging from 6.5 to 2.0 mm as labelled; (b) hard dough, feed thickness = 5.3 mm, exit thickness ranging from 4.9 to 2.0 mm as labelled.

dough, the two rolling parameters rise approximately linearly at a rate equivalent to 0.4% per minute of ageing. Rolling experiments were typically completed using dough between 45 and 110 min old, and hence the ageing effect can be expected to have added a variation between data sets of up to 25%. For the hard dough, the average roll torque and roll separating force also appear to increase linearly with time. The trends represent a more pronounced ageing effect than that observed for the short dough, with an average increase in the parameters of about 2.5% per minute. However, for hard dough tested up to an age of 70 min, the average increase in rolling parameters was somewhat less, in the region of 0.7% per minute. This evidence suggests that the rate of change of the parameters slowed markedly with increasing dough age. In general, rolling experiments were performed 20 min after mixing, and all were complete within 1 h. The increase in roll torque and roll separating force due to ageing in these 40 min is therefore of the order of 20–30%. A given set of experiments generally took between 10 and 15 min, and hence ageing would contribute a spread of 10–20% to the data points.

Fig. 14 shows the results of experiments conducted to investigate the effect of roller speed on the roll torque and separating force. In general, there is an increase in the rolling parameters of about 40–50% for both doughs as the speed increases from 2 to 30 rpm. Whilst there is some scatter in the data, the trends qualitatively reflect the non-linear velocity dependence of the die entry pressures as shown in Figs. 2(a) and 6(a).

Control over the temperature of the rolling laboratory was limited, and so it was not possible to investigate the effect of dough temperature for the rolling process explicitly. The short dough experiments were performed at temperatures between 16 and 26 °C, and those with hard dough at 21–25 °C. However, with dough ageing, experimental error and the variation between material batches all contributing to scatter in the results, it was not possible to quantify the effect of such temperature ranges.

4. Modelling

4.1. Plasticity-based model: Orowan's hot metal rolling model

To model the behaviour of doughs using plasticity theory, it is necessary to take account of their strain rate dependence. Orowan's hot metal rolling model is formulated so that strain or strain rate dependence of the shear yield stress can be incorporated. In the Benbow–Bridgwater characterisation of strain rate dependent

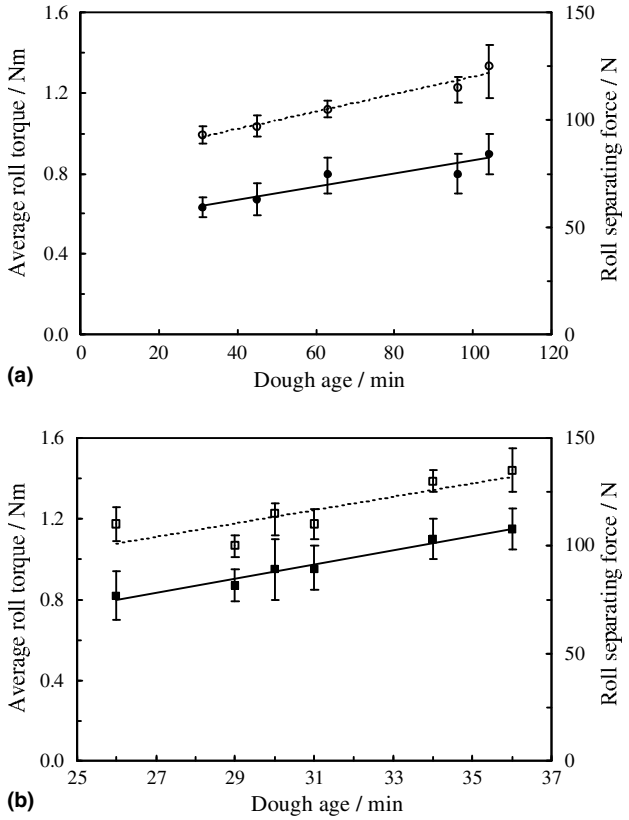

Fig. 13. Average roll torque (closed symbols) and roll separating force (open symbols) sensitivity to dough age at 6 rpm for (a) short dough, feed thickness 3.8 mm, exit thickness 2.2 mm, and (b) hard dough, feed thickness 6.9 mm, exit thickness 4.0 mm. Solid and dotted lines represent best fit linear trendlines.

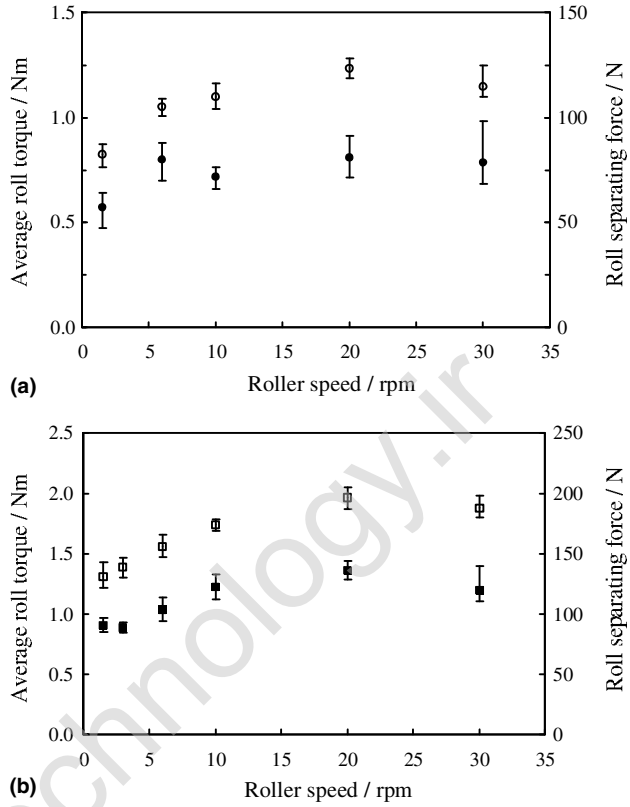

Fig. 14. Average roll torque (closed symbols) and roll separating force (open symbols) sensitivity to roller speed for (a) short dough, feed thickness 3.8 mm, exit thickness 2.2 mm, and (b) hard dough, feed thickness 5.5 mm, exit thickness 3.8 mm.

materials, the mean extrudate velocity in the die land is used as an indicator of the strain rate in the die entry region. However, the Benbow–Bridgwater α and m velocity terms are too specific to ram extrusion to be applied directly to rolling. It is necessary to transform them so that they describe a strain rate dependence more explicitly. Zheng, Carlson, and Reed (1992) reported that V should be replaced with (V/D) after experimenting with a numerical simulation of the flow of a power law fluid through a square entry contraction. The mean extensional strain rate is found to be independent of the shape of the deformation zone profile and dependent only on its length (Steffe, 1992). Assuming the deformation zone during ram extrusion has the length of a conical die entry region with an entry angle of 45°, or just under half the barrel diameter, then when evaluated for an entry diameter of D_0 and a die land diameter of D, the mean strain rate is given by

$$\bar{\dot{\varepsilon}} = \frac{1}{L}\frac{4Q}{\pi}\left(\frac{1}{D^2} - \frac{1}{D_0^2}\right) \tag{20}$$

Evaluated for the extrusion geometry used for the characterisations and the estimate of deformation zone length, this may be expressed as

$$\bar{\dot{\varepsilon}} = 0.27\frac{V}{D} \tag{21}$$

This is equivalent to mean strain rates of up to about $5\ s^{-1}$. In order to insert this expression into the Benbow–Bridgwater equation for the entry region, the die entry pressure drop term is transformed to the following:

$$P_0 = 2\left(\sigma_0 + \alpha'\left[\frac{V}{D}\right]^m\right)\ln\left(\frac{D_0}{D}\right) \tag{22}$$

where the strain rate factor, α', is related to the Benbow–Bridgwater velocity factor by

$$\alpha' = \alpha D^m \tag{23}$$

Combining Eqs. (21)–(23) gives an expression for the strain rate adjusted die entry uniaxial shear stress, σ_0', which can be applied to rolling:

$$\sigma_0' = \sigma_0 + \alpha'\left[\frac{\bar{\dot{\varepsilon}}}{0.27}\right]^m \tag{24}$$

In order to replace the yield stress used in Orowan's model by this expression, an estimate of the mean strain rate during rolling must be obtained. In the plane strain of rolling, an equivalent statement of the strain rate is the rate at which the thickness of the rolled sheet

decreases in relation to its current thickness (Chakrabarty, 1987). Peck et al. (in press) hence reported that the strain rate during rolling may be expressed as

$$\dot{\varepsilon} = \frac{2H_0\omega R\sin\phi}{H^2\cos\phi} \tag{25}$$

where ω is the angular velocity of the rollers, and H is the sheet thickness. The mean strain rate for rolling is then obtained from

$$\bar{\dot{\varepsilon}} = \frac{1}{\phi_e - \phi_f}\int_{\phi_f}^{\phi_e} \dot{\varepsilon}\,\mathrm{d}\phi \tag{26}$$

where ϕ_e is the exit angle of the sheet. When evaluated this indicates that the rolling experiments featured mean strain rates of up to 6 s^{-1}. In the forthcoming comparisons this expression is evaluated for each test and the yield shear stress, k, given by the left hand side of Eq. (19), is modified for strain rate effects via Eq. (24).

4.1.1. Short dough

Fig. 15 shows the experimental and predicted roll torques and separating forces for short dough sheets of feed thickness 3.7 mm. The strain rate modification has a pronounced effect on the model predictions at 1.5, 6 and 20 rpm. Table 1 identified a number of different plausible parameter sets describing the die entry region behaviour of short dough. The current analysis has been illustrated using σ_0 values of 0.04 and 0.16 MPa, in order to investigate the extent of the difference between the two descriptions of the material. The results are relatively disappointing. The experimental data tend to lie between the model predictions that employ the two yield stress values, but before the strain rate dependent terms have been added.

4.1.2. Hard dough

Roll torque and separating force results are shown in Fig. 16 for hard dough sheets of feed thickness 3.7 mm. The strain rate modified plasticity exerts a similarly pronounced effect on the model predictions as for the short dough. Again, the strain rate terms do not appear to be an appropriate description of the rolling process. Model predictions using yield stresses of 0.04 and 0.24 MPa (Table 1) with no strain rate dependence tend to bracket the experimental data, but when the strain rate effect is included then the model over-predicts by a factor of about two to three.

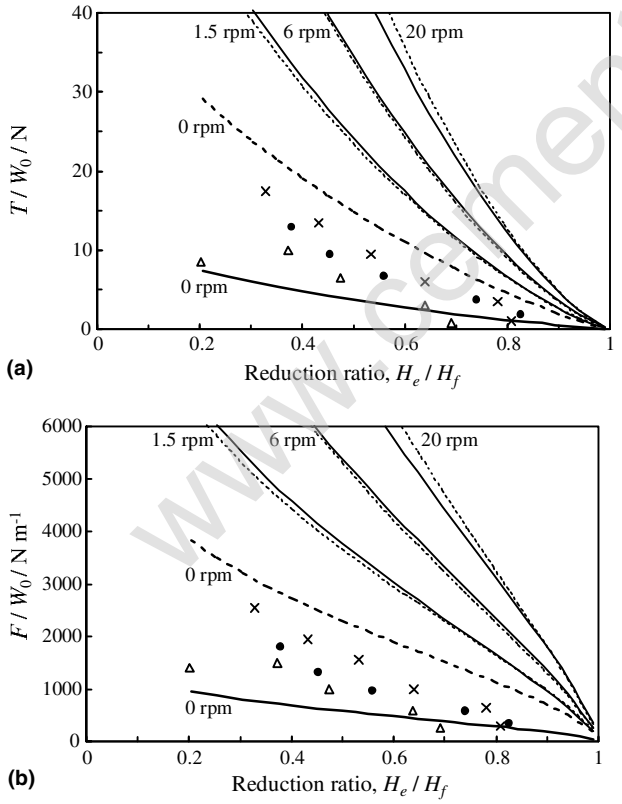

Fig. 15. Modelling short dough (feed thickness 3.7 mm) using strain rate dependent plasticity: (a) roll torque per unit width, and (b) roll separating force per unit width. Experimental data: (△) 1.5 rpm, (●) 6 rpm, and (×) 20 rpm. Model: solid lines for $\sigma_0 = 0.04$ MPa, dotted lines for $\sigma_0 = 0.16$ MPa, for roller speeds as labelled.

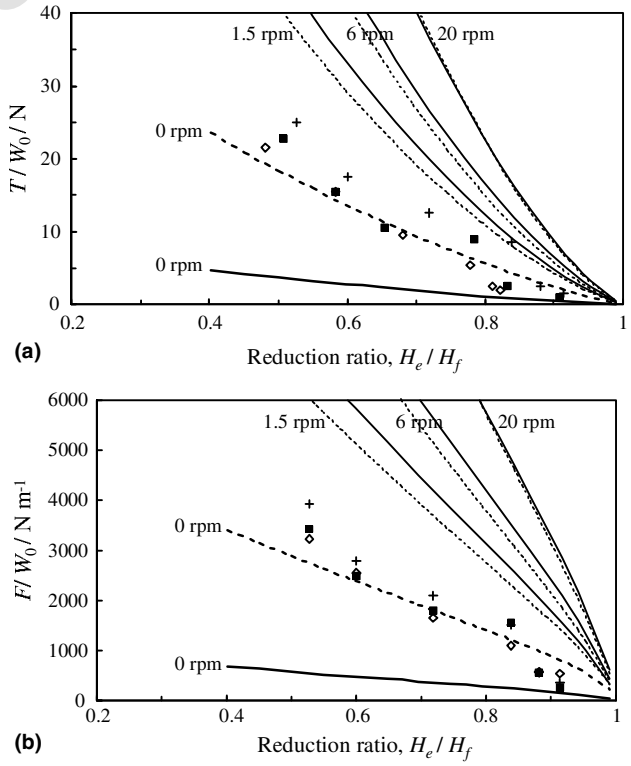

Fig. 16. Modelling hard dough (feed thickness 3.7 mm) using strain rate dependent plasticity: (a) roll torque per unit width, and (b) roll separating force per unit width. Experimental data: (◇) 1.5 rpm, (■) 6 rpm, and (+) 20 rpm. Model: solid lines for $\sigma_0 = 0.04$ MPa, dotted lines for $\sigma_0 = 0.16$ MPa, for roller speeds as labelled.

4.2. Fluid mechanics modelling: power law fluids without slip

Eqs. (14)–(16) summarise the power law sheeting model of Levine, and the results of the numerical integration required for the calculation of the force, torque and pressure predictions have been reported in the literature (Levine & Drew, 1990). These published solutions have been applied to the current experimental data, and polynomial approximations to Levine's parameters were devised and evaluated using spreadsheet software. The published solutions make application of the model convenient, but are restricted to values of λ of between 0.1 and 1, and for a fractional product thickness of 0.1–1.0.

Descriptions of both the shear and extensional properties of the two doughs were obtained from the ram extrusion data, on the assumption that the materials were not slipping against the wall of the die land. The calendering analysis upon which Levine's model is based employs the Reynolds lubrication approximations. The flows to which it is applicable are therefore dominated by shear, and thus require use of parameters describing shear response. The curvature of the roller is assumed to be slight and so extension will play only a minor role. In practice the response of the doughs is expected to be some combination of the extensional and shear components. If the parameters to be used are appropriate, then the extensional component of the deformation not represented in the model is expected to cause the model to underestimate the observed loads.

Section 1.2 described how the analysis allows for swelling of the sheet beyond the nip before the sheet detaches from the roller. The predictions made here are therefore based on the feed sheet thickness and the nip height. Predictions of the product sheet thickness have been generated and compared with the experimental results.

4.2.1. Short dough

A typical example of the performance of the Levine model using the short dough power law shear response parameters from Table 3 is shown in Fig. 17. These plots show the predicted and observed roll torques and separating forces for 3.7 mm thick feed sheets. It can be seen that for small sheet reductions, for which the model should be more appropriate, it underpredicts by a factor of 2 or more. It is proposed that the extensional response of the materials, which is not represented in the shear response parameters required by the model, is likely to be causing the discrepancy. However, the model has captured the spread in the force and torque results with changing roller speed. The predicted pressure profiles for two of these sheets are compared with the experimental data in Fig. 18(a) and (b), and the model is seen to underpredict the results. Taking an

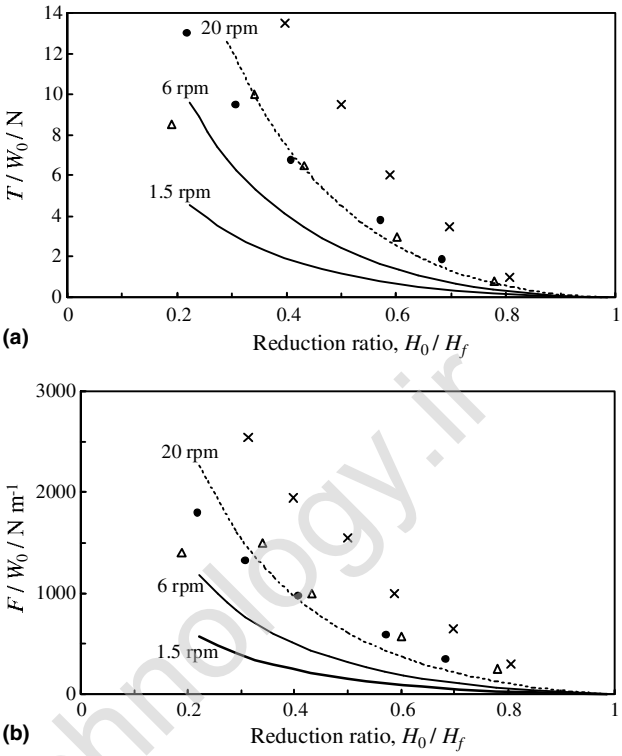

Fig. 17. Modelling short dough (feed thickness 3.7 mm) using power law fluid model: (a) roll torque per unit width, and (b) roll separating force per unit width. Experimental data: (△) 1.5 rpm, (●) 6 rpm, and (×) 20 rpm. Model: lines for roller speeds as labelled.

average over all the experiments, the predicted product sheet thickness was 10% greater than the nip height. This is slightly larger than observed; on average the product sheets were about 6% larger than the nip.

4.2.2. Hard dough

A sample of the Levine model predictions for hard dough, using the values from Table 3, is shown in Fig. 19. The predictions are 3–4 times lower than the experimental values. However, the lower power law flow index ($\lambda = 0.25$) is reflected in the smaller spread in the experimental data with changing roller speed, and the model also performs well in predicting the product sheet thickness; the 6% average increase beyond the nip matches the experimental results. Pressure profiles are included in Fig. 18(c) and (d), and the model once again underpredicts the response.

4.3. Fluid mechanics modelling: apparent power law description

The underpredictions of the power law based fluid mechanics model are in contrast to those provided by the modified plasticity approach. This latter analysis used data from the die entry region of extrusion rather than from the capillary flow of the die land. In the die

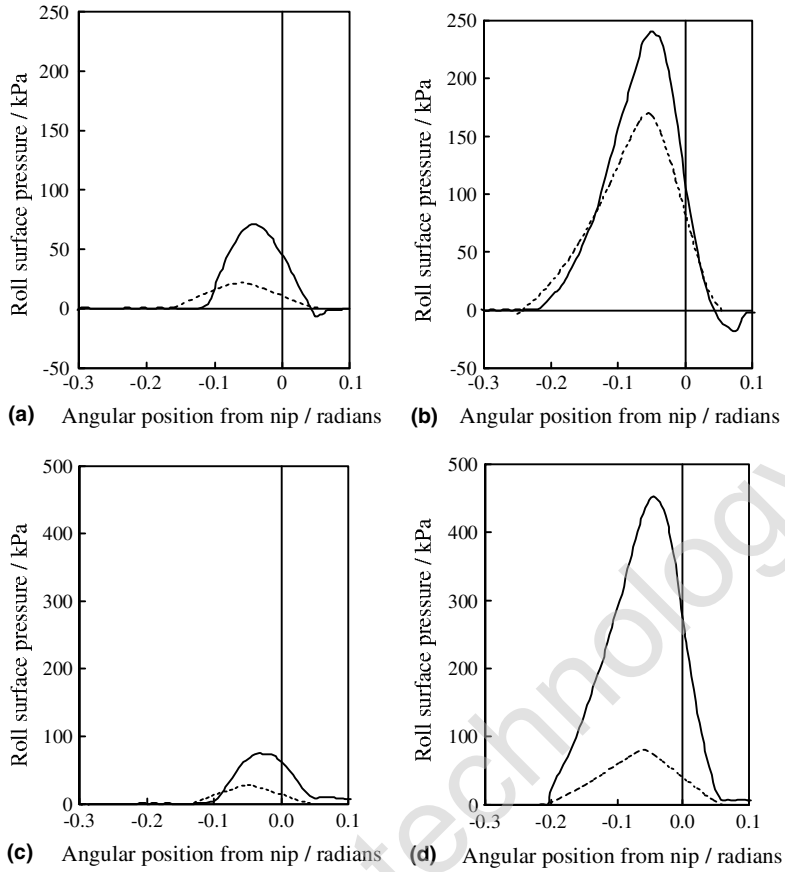

Fig. 18. Roll surface pressure profiles (sheet feed thickness 3.7 mm, roller speed 6 rpm) for short dough with exit sheet thickness of (a) 3.1 mm and (b) 1.4 mm, and for hard dough with exit sheet thickness of (c) 3.1 mm and (d) 1.9 mm. Solid lines = experiment, dotted lines = power law fluid model.

entry region of the ram extrusion tests, the material is undergoing a large reduction in cross-sectional area (over 98%), and so its extensional response will be governing the extrusion behaviour. It is therefore not surprising to find that the plasticity model is predicting larger values than those predicted by the power law based fluid mechanics model.

The contrast between the extensional and shear responses seems such that neither the shear description, nor a predominantly extensional description, are able to describe rolling adequately. Therefore, an empirical power law description of the materials to describe the rolling experiments is now found. Eq. (15) predicts the roll separating force to be proportional to the roll surface speed raised to the power λ, the effective power law flow index. A plot of the logarithm of roll separating force versus the logarithm of roll surface speed would therefore yield a straight line with a gradient equal to λ if a power law description is appropriate. The data are plotted in this form in Fig. 20. The data in the figure are taken from experiments in which the roll speed was systematically altered with no change in rolling geometry. As can be seen, the data fit a straight line, with effective power law flow indices of 0.19 for short dough and 0.22 for hard dough. For hard dough there is reasonable agreement with the proposed shear and extensional indices of 0.25 ± 0.12 (Table 3) and 0.26 ± 0.03 (Table 4) respectively. The shear response of the short dough was estimated in the capillary analysis as $\lambda = 0.5$ (Table 3). This does not agree with the value above, which is closer to the extensional response of 0.24 ± 0.04 (Table 4), indicating that the extensional response of the material is an important component of the deformation.

From Eq. (14), a plot of the logarithm of roll torque against the logarithm of roll surface speed should also yield a straight line with a gradient equal to λ in the Levine model. Thus for short dough the λ value is found to be smaller (0.15) than that obtained from the roll separating force, whilst for hard dough it is larger (0.24). For each dough, the average of the two effective indices has been applied to the equations predicting roll torque and separating force. The fact that the doughs deviate from descriptions of power law fluids becomes evident, in that it is not possible to find values for K, the power law fluid consistency, to satisfy all the experimental results simultaneously. To illustrate, the average of the effective flow indices was used and the value of K was found that minimised the square of the fractional

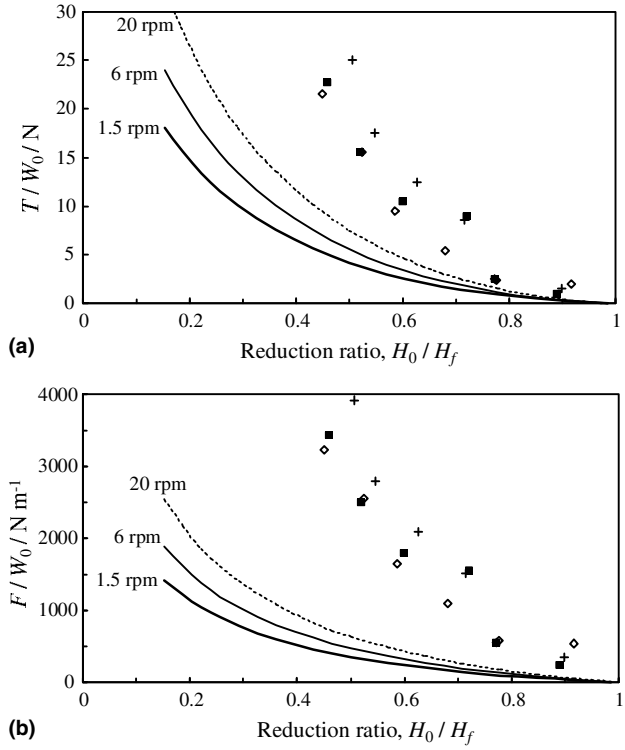

Fig. 19. Modelling hard dough (feed thickness 3.7 mm) using power law fluid model: (a) roll torque per unit width, and (b) roll separating force per unit width. Experimental data: (◇) 1.5 rpm, (■) 6 rpm, and (+) 20 rpm. Model: lines for roller speeds as labelled.

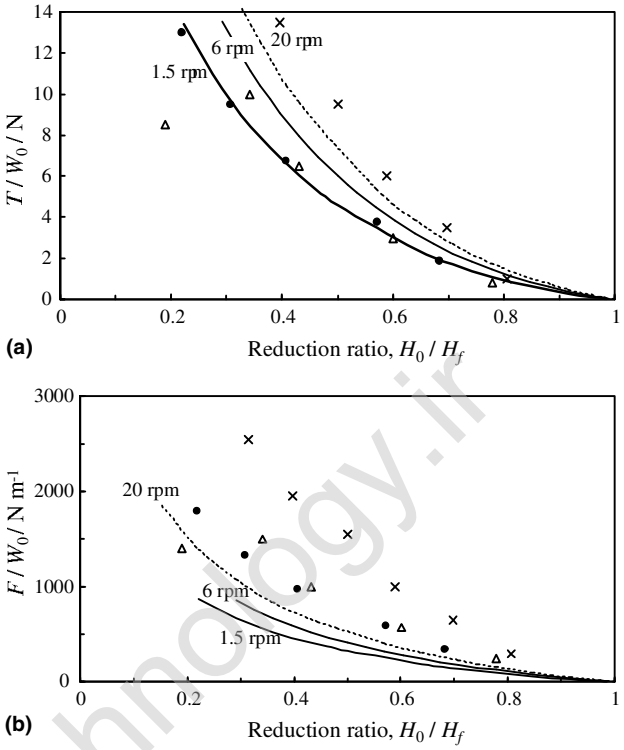

Fig. 21. Modelling short dough (feed thickness 3.7 mm) using fluid model with optimised power law description ($K = 6.4$ kPa s^{λ}, $\lambda = 0.17$): (a) roll torque per unit width, and (b) roll separating force per unit width. Experimental data: (△) 1.5 rpm, (●) 6 rpm, and (×) 20 rpm. Model: lines for roller speeds as labelled.

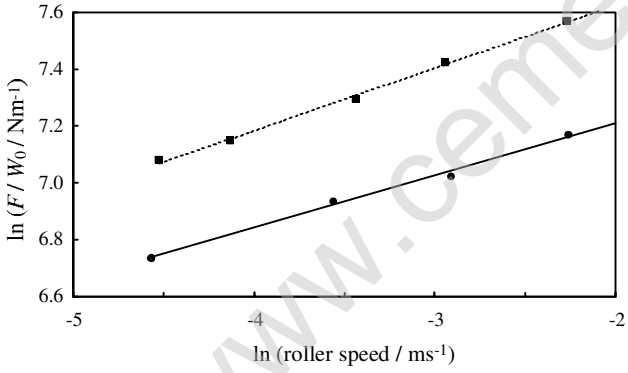

Fig. 20. Plot of logarithm of roll separating force per unit width against logarithm of roller speed: (●) short dough, feed thickness 4.0 mm, exit thickness 2.2 mm; (■) hard dough, feed thickness 5.5 mm, exit thickness 3.5 mm. Lines indicate best fit linear trendlines.

difference in both roll torque and separating force between the model and all the experimental results. The effective power law consistencies thus generated were 6.4 and 18.3 kPa s^{λ} for short and hard doughs respectively.

The resulting predictions for 3.7 mm feed sheets are shown in Figs. 21 and 22 for short and hard dough respectively. For both materials, the agreement between model and experimental data is good for the roll torque, but the roll separating force is underpredicted. The corresponding pressure profiles for two sheet sizes are included in Fig. 23. The predictions for the short dough are similar to those generated using the original Levine model (Fig. 18), whereas those for the hard dough show better agreement. It is evident that the optimal power law description depends on the deformation geometry. This suggests either that the balance of shear and extensional work is shifting as the geometry changes, and/or that a power law description of the materials is inadequate. In particular, the yield stress behaviour of the materials is one indication that they do not behave entirely as power law fluids. It is therefore not surprising that the Levine model cannot describe these materials satisfactorily.

5. Conclusions

The rolling of contrasting biscuit doughs, viz. a short dough and a hard dough, has been investigated. Two commonly reported approaches for characterising and modelling soft-solid materials have been implemented. The doughs were characterised by analysing data from capillary extrusion experiments. A Benbow–Bridgwater characterisation of the die entry region generated die

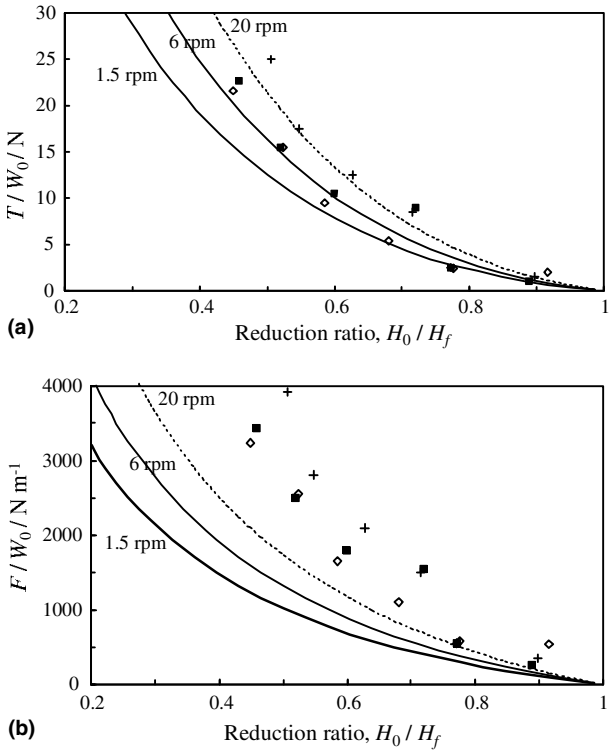

Fig. 22. Modelling hard dough (feed thickness 3.7 mm) using fluid model with optimised power law description ($K = 18.3$ kPa s$^{\lambda}$, $\lambda = 0.23$): (a) roll torque per unit width, and (b) roll separating force per unit width. Experimental data: (◇) 1.5 rpm, (■) 6 rpm, and (+) 20 rpm. Model: lines for roller speeds as labelled.

entry parameters that were sufficient for the roll torques and separating forces to be predicted using a strain rate modified plasticity model. However, the agreement of this model with the doughs was poor, with the predicted strain rate dependence being too great. The range of plausible values for the yield stress alone tended to bracket the experimental data without addition of the strain rate dependent terms. Since the Benbow–Bridgwater characterisation method proved to be poorly suited to these materials, a power law rheology capillary analysis of the extrusion data was also performed. This analysis examined the doughs in terms of shear and extensional components, and relies on the material in the die land being in a state of internal shear. If this assumption were correct, then the analysis indicated that deformation of these doughs would be dominated by extensional strains. This is consistent with their complex structure, particularly for the highly developed gluten network in the hard dough.

The rolling of the doughs was modelled using the frequently cited analysis of Levine incorporating a power law rheology. Since it is formulated only in terms of material shear, the shear components of the power law fluid characterisation were used in the calculations. The model predictions were too low. It is proposed that this is because the model does not make allowance for the complexities of materials which require separate extensional and shear strain descriptions. In particular, the high extensional viscosities of the doughs would act to increase the measured roll torque and separating force, in line with observations. In recognition of these problems, empirical relationships were determined which would describe the rolling experiments adequately. However, the materials' deviation from a power law based description became evident from the impossibility of generating power law parameters to satisfy both the torque and force comparisons simultaneously. The parameters were found to be dependent upon the deformation geometry. Hence the predictions of roll separating force were consistently too low.

Some of the general observations are not reflected in the model predictions, and are unlikely to be observed in rolling of the metal and polymer industries. For example, in 15% of the experiments with short dough, the sheet disintegrated or fractured. Also, as the sheet reduction ratio increased, a double pressure peak was observed, which is thought to be due to the development of a recirculation zone within the dough. The double pressure peak was not observed in the rolling of hard dough. Another highlighted feature was that of sheet adhesion to the rollers, which was captured by the roll surface pressure transducer. Small negative pressure peaks were sometimes observed as the short dough sheet detached from the rollers. Also of note was the large proportion of product sheets that adhered to a roller surface. It is unclear why this happened. For the hard dough, only two sheets detached even though the sheets were insufficiently adhesive to produce negative pressures. The only conclusion that may be drawn from the available evidence is that the adhesive force between roller and sheet is consistently strong enough to overcome sheet rigidity. This is unsurprising for the thinner sheets.

Whilst the quantity of experimental data provided several observations of interest, dough ageing and temperature variation affected the experimental data. Although their influences were quantified in experiments in the ram extruder, their effects could not be dissociated from other variables. The comparison between different sets of results and the quality of the comparisons with the modelling work would have been improved if the number of experiments had been reduced but with the age of the dough fixed. Ambient temperature is more difficult to control, but its variation must be eliminated if scatter in experimental results is to be reduced.

The development of an analysis of dough rolling including shear and extensional deformation terms has been identified as an area that would benefit most from further work. This is likely to require a finite element solution, such as that developed by Levine, Corvalan, Campanella, and Okos (2002). The characterisation of

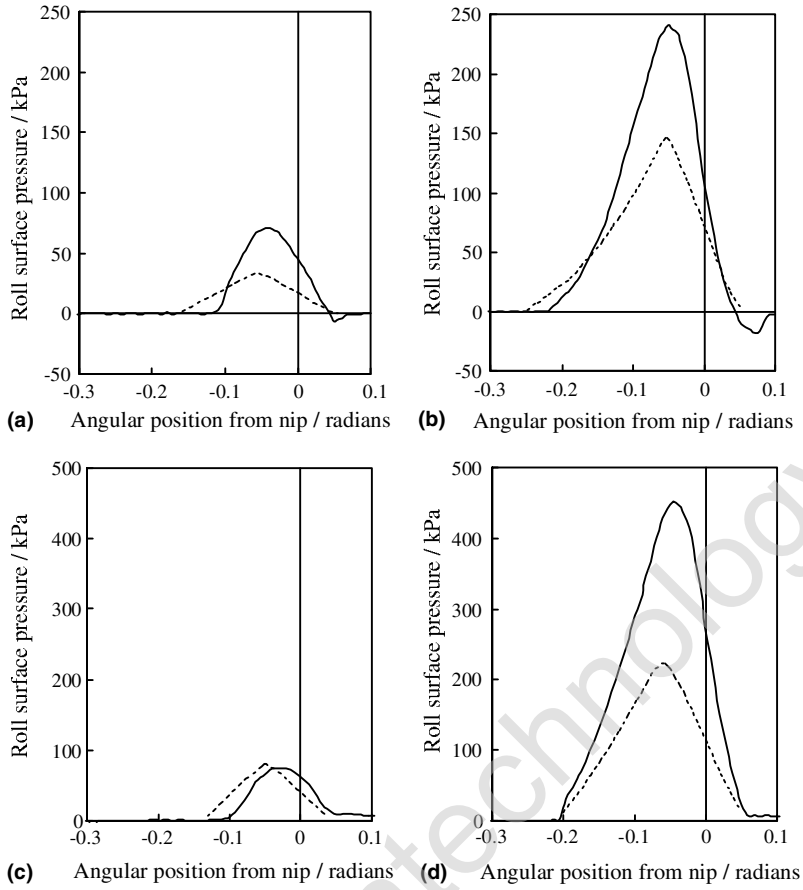

Fig. 23. Roll surface pressure profiles (sheet feed thickness 3.7 mm, roller speed 6 rpm) for short dough with exit sheet thickness of (a) 3.1 mm and (b) 1.4 mm, and for hard dough with exit sheet thickness of (c) 3.1 mm and (d) 1.9 mm. Solid lines = experiment, dotted lines = apparent power law fluid model.

the doughs requires further work for full use to be made of a more complete model of the operation. The sheet-roller adhesion phenomenon underpins a range of industrially important processes, such as rotary moulding.

Acknowledgement

A studentship for MCP from the EPSRC and support from United Biscuits R&D (High Wycombe, UK) are gratefully acknowledged.

References

Adams, M. J., Biswas, S. K., Briscoe, B. J., & Kamyab, M. (1991). The effect of interface constraints on the deformation of pastes. *Powder Technology, 65*, 381.

Benbow, J. J., Lawson, T. A., Oxley, E. W., & Bridgwater, J. (1989). Prediction of paste extrusion pressure. *Ceramic Bulletin, 68*, 1821.

Benbow, J. J., & Bridgwater, J. (1993). *Paste flow and extrusion*. Oxford, UK: Clarendon Press.

Bennion, M. (1980). *The science of food*. New York, USA: John Wiley & Sons.

Castell-Perez, M. E. (1992). Viscoelastic properties of dough. In M. A. Rao & J. F. Steffe (Eds.), *Viscoelastic properties of foods*. London, UK: Elsevier Science Publishers.

Chakrabarty, J. (1987). *The theory of plasticity*. McGraw-Hill BookCompany.

Cheyne, A., Barnes, J., & Wilson, D. I. (2005). Extrusion behaviour of cohesive potato starch pastes: I. Rheological characterisation. *Journal of Food Engineering, 66*, 1.

Chung, T. (1983). Analysis of the calendering of compressible fluids. *Journal of Applied Polymer Science, 28*, 2119.

Gisslen, W. (2001). *Professional baking*. New York, USA: John Wiley & Sons.

Horrobin, D. J. (1999). Theoretical aspects of paste extrusion. PhD Thesis. UK: University of Cambridge.

Kiparissides, C., & Vlachopoulos, J. (1978). The study of viscous dissipation in the calendering of power law fluids. *Polymer Engineering and Science, 18*, 210.

Levine, L. (1983). Estimating output and power of food extruders. *Journal of Food Process Engineering, 6*, 1.

Levine, L. (1985). Throughput and power of dough sheeting rolls. *Journal of Food Process Engineering, 7*, 223.

Levine, L. (1996). Model for the sheeting of dough between rolls operating at different speeds. *Cereal Foods World, 41*(8), 690.

Levine, L., & Drew, B. A. (1990). Rheological and engineering aspects of the sheeting and laminating of doughs. In H. M. Faridi & J. M. Faubion (Eds.), *Dough rheology and baked product texture*. New York, USA: Van Nostrand Reinhold.

Levine, L., Corvalan, C. M., Campanella, O. H., & Okos, M. R. (2002). A model describing the two-dimensional calendering of finite width sheets. *Chemical Engineering Science, 57*, 643.

Manohar, R. S., & Rao, P. H. (1997). Effect of mixing period and additives on the rheological characteristics of dough and quality of biscuits. *Journal of Cereal Science, 25*, 197.

Middleman, S. (1977). *Fundamentals of polymer processing*. McGraw Hill Book Company.

Mitsoulis, E., Vlachopoulos, J., & Mirza, F. A. (1985). Calendering analysis without the lubrication approximation. *Polymer Engineering and Science, 25*(1), 6.

Orowan, E. (1943). The calculation of roll pressure in hot and cold flat rolling. *Proceedings of the Institute of Mechanical Engineers, 150*, 140.

Ovenston, A., & Benbow, J. J. (1967). Effects of die geometry on the extrusion of clay-like material. *Transactions of the British Ceramic Society, 11*, 543.

Peck, M. C. (2002). Roller extrusion of pastes. PhD Thesis, UK: University of Cambridge.

Peck, M. C., Rough, S. L., & Wilson, D. I. (in press). Roller extrusion of a ceramic paste. *Industrial & Engineering Chemistry Research and Designing*.

Podmore, J. (1994). Fats in bakery and kitchen products. In D. P. J. Moran & K. K. Raja (Eds.), *Fats in food products*. Glasgow, UK: Chapman & Hall.

Rao, M. A. (1992). Classification, description and measurement of viscoelastic properties of solid foods. In M. A. Rao & J. F. Steffe (Eds.), *Viscoelastic properties of foods*. London, UK: Elsevier Science Publishers.

Rough, S. L., Bridgwater, J., & Wilson, D. I. (2000). Effects of liquid phase migration on extrusion of microcrystalline cellulose pastes. *International Journal of Pharmaceutics, 204*, 117.

Steffe, J. F. (1992). *Rheological methods in food process engineering*. East Lansing, USA: Freeman Press.

Zheng, J., Carlson, W. B., & Reed, J. S. (1992). Flow mechanics of extrusion through a square-entry die. *Journal of the American Ceramic Society, 75*, 3011.